Grouping of Spindle Activity during Slow Oscillations in Human Non-Rapid Eye Movement Sleep

Matthias Mölle, Lisa Marshall, Steffen Gais, and Jan Born

Institute of Neuroendocrinology, University of Lübeck, 23538 Lübeck, Germany

Based on findings primarily in cats, the grouping of spindle activity and fast brain oscillations by slow oscillations during slow-wave sleep (SWS) has been proposed to represent an essential feature in the processing of memories during sleep. We examined whether a comparable grouping of spindle and fast activity coinciding with slow oscillations can be found in human SWS. For negative and positive half-waves of slow oscillations (dominant frequency, 0.7–0.8 Hz) identified during SWS in humans ($n = 13$), wave-triggered averages of root mean square (rms) activity in the theta (4–8 Hz), alpha (8–12 Hz), spindle (12–15 Hz), and beta (15–25 Hz) range were formed. Slow positive half-waves were linked to a pronounced and widespread increase in rms spindle activity, averaging 0.63 ± 0.065 μV (23.4%; $p < 0.001$, with reference to baseline) at the midline central electrode (Cz). In contrast, spindle activity was suppressed during slow negative half-waves, on average by −0.65 ± 0.06 μV at Cz (−22%; $p < 0.001$). An increase in spindle activity 400–500 msec after negative half-waves was more than twofold the increase during slow positive half-waves ($p < 0.001$). A similar although less pronounced dynamic was observed for beta activity, but not for alpha and theta frequencies. Discrete spindles identified during stages 2 and 3 of non-rapid eye movement (REM) sleep coincided with a discrete slow positive half-wave-like potential preceded by a pronounced negative half-wave ($p < 0.01$). These results provide the first evidence in humans of grouping of spindle and beta activity during slow oscillations. They support the concept that phases of cortical depolarization during slow oscillations, reflected by surface-positive (depth-negative) field potentials, drive the thalamocortical spindle activity. The drive is particularly strong during cortical depolarization, expressed as surface-positive field potentials.

Key words: slow oscillations; spindle activity; human; sleep; EEG; cortical depolarization

In recent years, studies in humans and animals have accumulated converging evidence for the hypothesis that a reprocessing of events acquired during previous wakefulness occurs during non-rapid eye movement (REM) sleep, which eventually supports long-term storage of respective neuronal representations (Plihal and Born, 1997; Buzsáki, 1998; Gais et al., 2000; Sutherland and McNaughton, 2000). At the level of rhythmic activity in the brain, spindle activity (12–15 Hz) and faster oscillatory activity have both been linked to aspects of the consolidation process (Siapas and Wilson, 1998; Steriade and Amzica, 1998; Destexhe et al., 1999; Sejnowski and Destexhe, 2000; Gais et al., 2002). Spindle oscillations provoke a massive Ca^{2+} entry into the spindling cortical cells, and thus could set the stage for plastic synaptic changes that are supposed to be induced during subsequent slow-wave activity. Notably, spindle and fast oscillatory activity in cats have been found to be distinctly grouped by slow (<1 Hz) oscillations (Contreras and Steriade, 1995, 1996; Contreras et al., 1997; Steriade and Amzica, 1998; Steriade, 1999). Moreover, the grouping by slow oscillations has been considered relevant for the effective generation in particular of spindle activity and for establishing reiterative processing of memories in non-REM sleep. At the cellular level, the slow oscillations are built up by the rhythmic sequence of membrane depolarization and hyperpolarization of cortical pyramidal neurons, with the depolarization associated with depth-negative and surface-positive EEG field potentials and, conversely, the hyperpolarizing phase associated with a depth-positive, surface-negative EEG potential (Steriade et al., 1994; Contreras and Steriade, 1995). Spindle activity originating within thalamo-neocortical loops and also faster frequencies were found to be driven during the depolarizing (surface-positive) phase of slow waves, during which the firing of pyramidal cells is increased. In contrast, the hyperpolarizing (surface-negative) phase is associated with neuronal silence (Buzsáki et al., 1988; Contreras and Steriade, 1995; Steriade et al., 1996; Destexhe et al., 1999).

A grouping of spindle activity by slow oscillations has been suggested also to be present in the human EEG (Achermann and Borbély, 1997; Amzica and Steriade, 1997). However, distinct slow rhythms for spindles were revealed at a periodicity of ~4 sec and slower (i.e., at a much longer periodicity than that of the slow oscillations displaying an obvious peak in humans and cats at ~0.7–0.8 Hz) (Achermann and Borbély, 1997; Marshall et al., 2000). Also, spindle activity is known to be generally decreased with increasing delta activity in humans, which could mask a grouping of this activity present during slow-wave sleep (SWS) (Aeschbach and Borbély, 1993; Dijk et al., 1993; De Gennaro et al., 2000a,b). Given the importance that has been ascribed to the regulation of spindle and fast oscillatory activity by slow oscillations during SWS for the possibility of memory processing during this seemingly quiet period of sleep, we examined the temporal dynamics between these faster rhythmic activities and slow oscillations during non-REM sleep and SWS in the human EEG, with particular reference to spindle activity. As in animals, we ex-

Received June 17, 2002; revised Sept. 23, 2002; accepted Sept. 27, 2002.

This work was supported by a grant from the Deutsche Forschungsgemeinschaft. We thank Dr. D. Contreras for helpful comments on a previous version of this manuscript.

Correspondence should be addressed to Dr. M. Mölle, Institute of Neuroendocrinology, University of Lübeck, Ratzeburger Allee 160, Haus 23a, 23538 Lübeck, Germany. E-mail: moelle@kfg.uni-luebeck.de.

 0270-6474/02/2210941-07$15.00/0

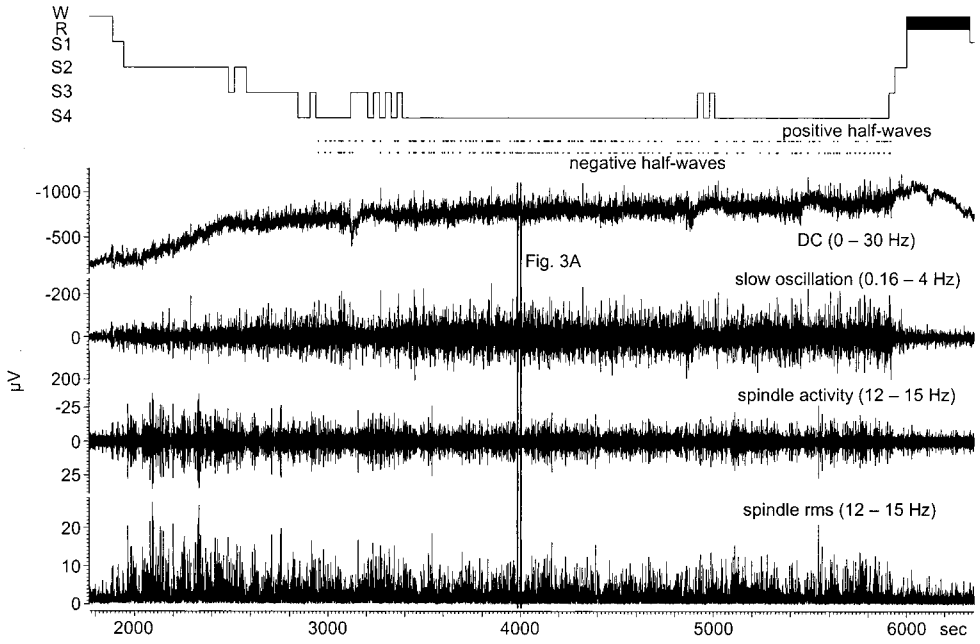

Figure 1. Selection of slow-oscillation half-waves. From *top* to *bottom*, Sleep hypnogram for the first cycle from an individual night (*W*, wake; *R*, REM sleep; *S1–S4*, non-REM sleep stages 1–4). *Dots* underneath indicate time points of the largest slow-positive and negative-oscillation half-waves chosen for analysis (see Materials and Methods for details). DC-recorded (0–30 Hz) original EEG signal, slow-oscillation signal (bandpass, 0.16–4 Hz), spindle activity (12–15 Hz), and spindle rms signal are shown. *Parallel vertical bars* indicate a critical 20 sec time interval used for the analyses as depicted in Figure 3*A*.

pected enhanced spindle activity during the depolarizing phase (i.e., surface-positive compared with surface-negative half-waves of slow oscillations).

MATERIALS AND METHODS

Subjects and EEG recordings. Direct current (DC) EEG signals were recorded from 13 young, healthy subjects (six females, seven males, aged 18–25 years) displaying regular sleep–wake rhythms and identified by interview as good sleepers. Because the present analyses relied on DC-recorded EEG signals and because restrained head movement is a necessary prerequisite for proper artifact-free recordings of this kind, subjects were asked to practice at home sleeping through two nights on their back wearing a cervical collar before the experiment proper. Only data from subjects who displayed normal sleep patterns on the experimental night were included in the analyses. In particular, care was taken that the first sleep cycle was well pronounced, revealed a minimum of artifacts, and possessed a minimum of at least 20 min of time spent in SWS [i.e., stages 3 and 4 according to the standard criteria by Rechtschaffen and Kales (1968)]. Recording of the DC potentials was as described previously (Marshall et al., 1998, 2000). In brief, recordings were obtained from electrodes located at F3, the midline frontal electrode (Fz), F4, C3, the midline central electrode (Cz), and C4 (international 10–20 system) referenced to linked mastoid electrodes. To attach the electrodes, clip-on sockets were fixed with collodion to the scalp (Bauer et al., 1989). Before filling sockets and electrodes with electrode gel (Electrode Electrolyte; TECA Corp., Pleasantville, NY), the underlying scalp was punctured with a sterile hypodermic needle, to eliminate possible skin potential artifacts (Picton and Hillyard, 1972). Electrode impedance was always <5 kohm. EEG signals were amplified (2000-fold) and analog-filtered (0–30 Hz) with a DC amplifier (Toennies DC/AC amplifier; Jaeger GmbH and Co., KG, Hoechberg, Germany). The DC offset was automatically corrected at a threshold of ±4 mV. With short-circuited input, the amplifier drift, if present, was <3 μV/hr. Analog DC/EEG signals were digitized at 100 Hz (CED 1401; Cambridge Electronics Design, Cambridge, UK) and stored on a personal computer for offline analysis.

Data analysis. Sleep stages (1, 2, 3, 4, and REM sleep), awake time, and movement artifacts were scored offline for 30 sec intervals (Rechtschaffen and Kales, 1968) (see Fig. 1). EEG data from the first sleep cycle were chosen, and analyses were targeted at channels Fz and Cz, where spindles and slow oscillations are most pronounced. (Analyses of the other channels did not add any substantial information.) To produce the slow-oscillation signal, first the DC shift was eliminated with a simple feedback filter, equivalent to a 6 dB/octave analog filter and a time constant of 1 sec (corresponding to 0.16 Hz). Subsequently, EEG data were digitally filtered with a low-pass finite impulse response (FIR) filter of 4 Hz (−3 dB at 4.7 Hz; −96 dB at ≥6 Hz). This bandpass filtering (0.16–4 Hz) was done after spectral power analysis of the EEG in all individuals; it revealed a single broad peak indicating maximum power at ~0.7 Hz (see Fig. 2). Exploratory analyses performed on a more narrow frequency band of slow oscillation of <1 Hz revealed essentially identical results.

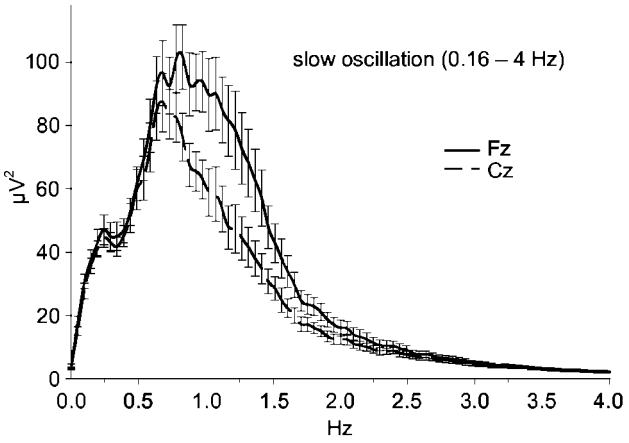

Figure 2. Averaged spectral power density for the slow oscillation frequency band (0.16–4 Hz) at Fz (*solid line*) and Cz (*dashed line*). Note the peak power density at 0.7–0.8 Hz.

To produce the spindle activity signal, a bandpass FIR filter of 12–15 Hz (−3 dB at 11.3 and 15.7 Hz; −96 dB from 0 to 10 Hz and at ≥17 Hz) was applied. After bandpass filtering, a root mean square (rms) signal was calculated with a time resolution of 0.05 sec using a time window of 0.1 sec (see Fig. 1). Basically, analog procedures were used to produce signals in the theta (4–8 Hz), alpha (8–12 Hz), and beta (15–25 Hz) frequency bands.

Two independent analyses were performed. For the first main analysis, the largest positive and negative half-waves were selected from SWS (stages 3 and 4) (see Fig. 3*A*) using a thresholding procedure applied to the slow-oscillation signal. This first analysis concentrated on wave-triggered averages. The calculation of wave-triggered averages consisted of averaging short windows of data (slow oscillatory activity and rms signal) time-locked to the positive and negative peaks of half-waves, which were numerically detected by a thresholding procedure in the slow-oscillation band signal. The peak time of a half-wave found was used for averaging if the following criteria were fulfilled: (1) The beginning

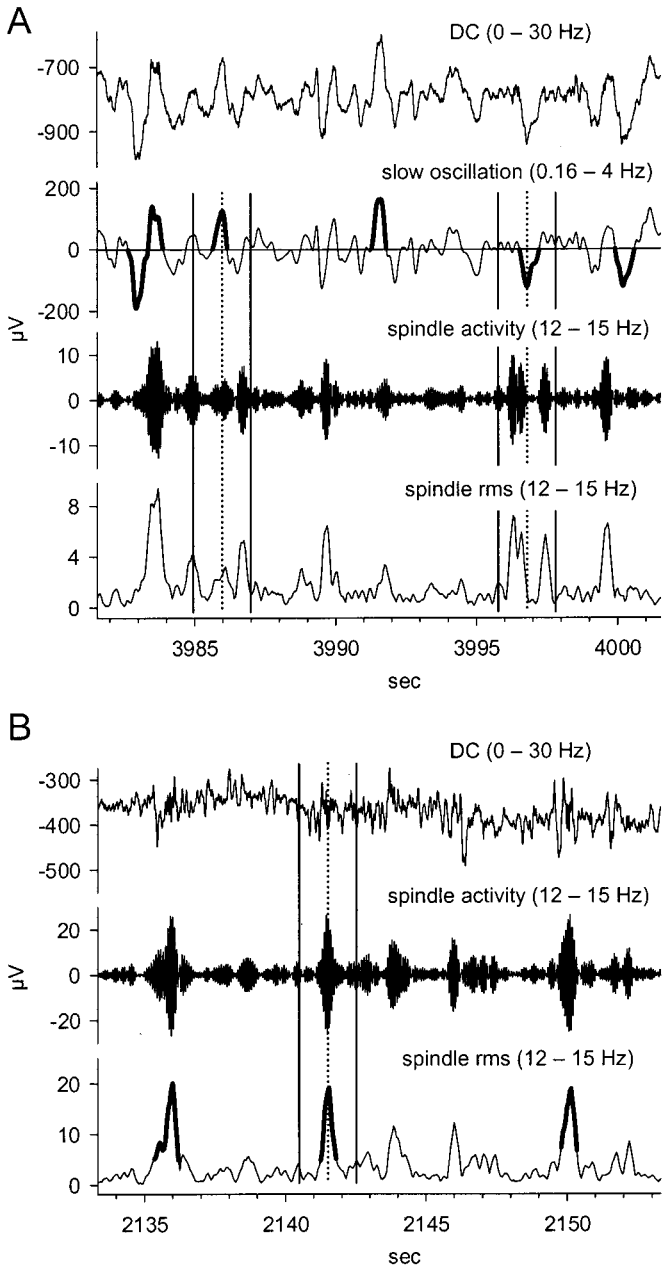

Figure 3. Steps of analysis illustrated for two 20 sec epochs of recordings for an individual subject (same as in Fig. 1). *A*, Analysis of slow oscillation-dependent changes in spindle activity. From *top* to *bottom*, DC-recorded (0–30 Hz) original EEG signal, slow oscillatory signal (0.16–4 Hz) with detected slow positive and negative half-waves indicated by a *thick solid line*, and spindle rms signal. For one positive and one negative half-wave each, the peak time used for time-locked averaging and the ±1 sec averaging interval are indicated by a *dotted line* and *two solid vertical lines*, respectively. *B*, Analysis of spindle-dependent changes in the DC potential, exemplified on discrete spindles that occurred during the first period of sleep stage 2 shown in Figure 1. From *top* to *bottom*, DC-recorded (0–30 Hz) original EEG during non-REM sleep stage 2, spindle activity filtered at 12–15 Hz, and spindle rms signal with identified spindle periods indicated by a *thick solid line*. Only the largest spindles were selected for analysis by a thresholding procedure applied to the spindle rms signal. For one spindle, the center time used for time-locked averaging and the ±1 sec averaging interval are indicated by a *dotted line* and *two solid vertical lines*, respectively.

Table 1. Mean number ± SEM of individually averaged data segments and thresholds used in the analyses of negative and positive half-waves and sleep spindles ($n = 13$)

	Fz	Cz
Negative half-waves		
Number	144.7 ± 10.7	122.4 ± 7.7
Threshold (μV)	148.5 ± 10.4	129.2 ± 7.3
Positive half-waves		
Number	115.7 ± 13.9	114.4 ± 8.1
Threshold (μV)	118.8 ± 7.7	108.5 ± 5.6
Sleep spindles		
Number	117.2 ± 10.0	121.8 ± 12.0
rms threshold (μV)	6.7 ± 0.5	7.3 ± 0.6

The thresholds for detecting negative and positive half-waves were applied at Fz and Cz to the slow oscillation signal (0.16–4 Hz). The thresholds for detecting sleep spindles were applied to the sigma rms signal (12–15 Hz).

and end of the half-wave were two succeeding zero-crossings of the slow-oscillation band signal separated from each other by 0.125–1 sec. (2) The peak amplitude between both zero-crossings exceeded a threshold of at least 80 μV and −80 μV for positive and negative half-waves, respectively. (3) The half-wave lay in a 30 sec epoch of sleep stage 3 or 4, which was free of movement artifacts. Threshold settings were such that in each case >50 half-waves were found. For all detected positive and negative half-waves, the slow-oscillation signal and the rms signal in the other frequency bands of interest were averaged with intervals of ±1.0 sec around the peak amplitude time. Grand mean averages across all 13 subjects were calculated.

It was also of interest to determine whether discrete spindles, typically most easily identified during non-REM sleep stage 2 in humans, are associated with slow oscillation-like shifts in the DC potential. For this second analysis, the largest sleep spindles were selected from sleep stages 2 and 3 (see Fig. 3*B*) using a thresholding procedure applied to the spindle rms signal. Thus, the second analysis concentrated on averages of the DC potential as triggered by discrete spindles. The respective calculation consisted of averaging short windows of data (spindle rms and DC potential) selected by reference of the time of occurrence of a sleep spindle. Sleep spindles were detected numerically using a thresholding procedure, comparable with the procedure of Schimicek et al. (1994), which searched for sleep spindles separately in the Fz and Cz channels. The center times of every detected sleep spindle were used to synchronize averaging, if the following criteria were fulfilled: (1) The beginning and end of a spindle were two succeeding threshold-crossings of the spindle rms signal separated by 0.4–1.3 sec. (2) The spindle rms signal between both threshold-crossings was larger than the threshold, which was determined individually for each subject, but in any case was >5 μV. (3) The spindle lay in a 30 sec epoch of sleep recordings free of artifacts. More than 50 spindles were found for each individual. For all spindles found, intervals of the DC potential (baseline corrected) and the spindle rms signal of ±1.0 sec around the spindle center were averaged, and grand mean averages across all 13 subjects were formed.

For a third analysis, individual cross-correlation functions between the potential of the slow oscillatory signal and the spindle rms signal were calculated during SWS. The slow oscillatory potential signal was downsampled to a time resolution of 0.05 sec. The two correlated time series began with the first 30 sec epoch of sleep stage 3 and ended with the last 30 sec epoch of sleep stage 4 within the first sleep cycle. The cross-correlation was calculated for time shifts up to ±2 sec (i.e., up to 80 points with an offset of 40 points).

RESULTS

Table 1 summarizes the number of averaged data segments and thresholds used for individual averaging in the analyses of negative and positive half-waves and sleep spindles. A relationship between slow-oscillation half-waves and spindle activity was already visible after superimposing epochs of EEG activity filtered in the spindle band for all positive and negative half-waves (Fig. 4*A*). Spindle activity is suppressed in a 200 msec interval around

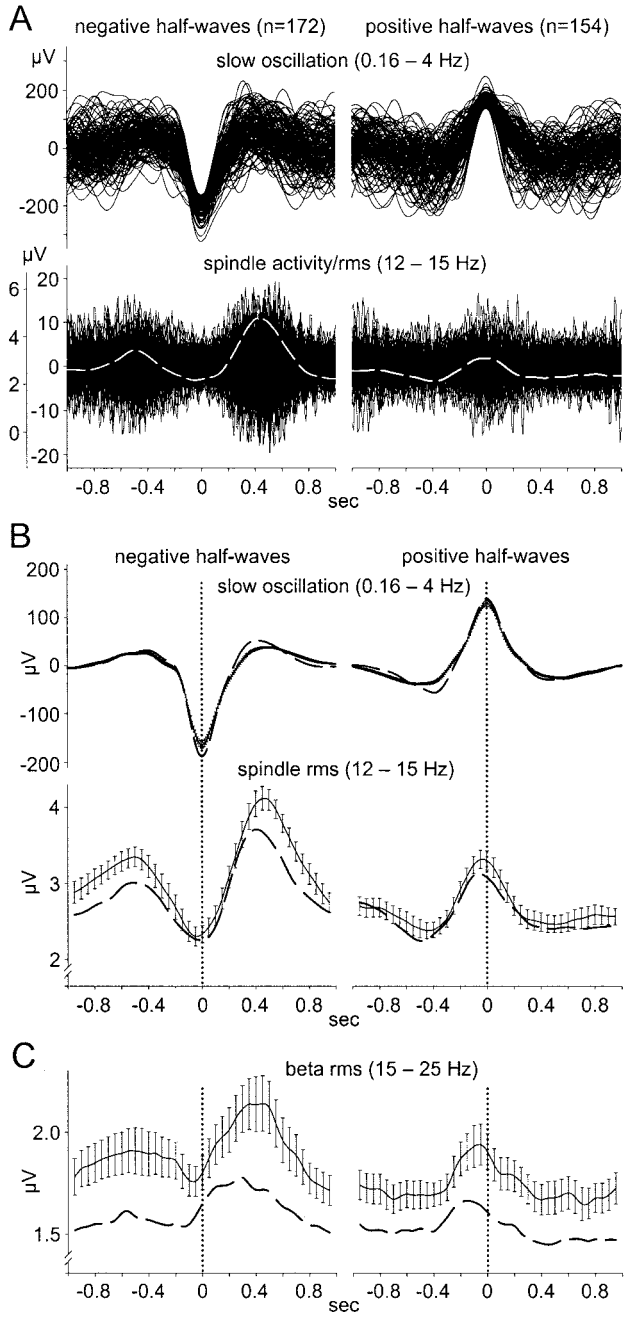

Figure 4. *A, top*, Superimposed slow negative (*left*) and positive (*right*) half-waves. *A, bottom*, Corresponding spindle band signals (*black line, right axis*) and mean spindle rms activity (*white dashed line, left axis*) in a single subject at Cz. *B*, Grand means (across 13 subjects) of results from wave-triggered analysis of slow negative (*left*) and positive (*right*) half-waves. The mean ± SEM slow-oscillation signal (*top*) and spindle rms signal (*bottom*) at Cz are shown. *Dashed lines* indicate mean values at Fz (without SEM). *C*, Grand means of beta rms signal. Note that the temporal dynamics of beta activity were similar to spindle activity, in particular at Cz. *Vertical dotted lines* indicate the half-wave peak time used for time-locked averaging.

the peak of negative half-waves and enhanced around the peak of positive half-waves. This relationship is most clearly seen in the grand means of half-wave-related spindle rms signals (Fig. 4B). The spindle rms value in both channels was on average 1 μV (i.e., 27.8 and 30.7% for Fz and Cz, respectively) lower during the peak of negative than during the peak of slow positive half-waves (Fz, 2.26 ± 0.16 vs 3.13 ± 0.15 μV; Cz, 2.30 ± 0.12 vs 3.32 ± 0.12 μV for negative and positive half-waves, respectively; $p < 0.001$). If the first 0.2 sec period of the averaged interval was defined as the baseline, then the decrease in spindle activity during negative half-waves was −0.37 ± 0.07 μV at Fz and −0.65 ± 0.06 μV at Cz ($p < 0.001$). The increase in spindle activity during positive half-waves was 0.41 ± 0.06 μV at Fz and 0.63 ± 0.09 μV at Cz ($p < 0.001$).

Interestingly, Figure 4*B* also reveals a distinct rebound enhancement after the negative half-wave-associated suppression of the spindle rms signal peaking ~400–500 msec after the lowest value. In both channels, the spindle rms value at this time was even higher than that during the peak of slow positive half-waves (0.58 ± 0.1 μV at Fz and 0.80 ± 0.12 μV at Cz; $p < 0.001$). Notably, the slow (positive) oscillatory potential at this time was ~100 μV lower than at the peak time of slow positive half-waves.

Changes in the rms signal for the adjacent beta frequency band (15–25 Hz) resulted in temporal dynamics similar to those seen for spindle activity (Fig. 4*C*). However, they were much less pronounced. The only consistent changes reaching significance were an increase in the beta rms signal during slow positive half-waves (Fz, 0.11 ± 0.04 μV; Cz, 0.21 ± 0.05 μV, with reference to baseline; $p < 0.05$) and, as seen only at Cz, the rebound increase in the rms signal after slow negative half-waves (0.37 ± 0.09 μV, with reference to the preceding trough; $p < 0.01$). The rms signals of the alpha (8–12 Hz) and theta (4–8 Hz) bands did not indicate any changes similar to that found for spindle activity. A significant increase ($p < 0.01$) in the rms signal for these two bands found selectively during the negative slope of slow negative half-waves reflects the fact that this amplitude decrement toward the negative peak is generally steeper than the changes toward positivity (also see Fig. 4*B*).

The analysis of spindle-triggered averages during sleep stages 2 and 3 revealed a complementary relationship between sleep spindles and the concurrently obtained DC potential (Fig. 5). When averaged time-locked to the center of spindles, the mean DC potential shows a distinct negative peak shortly before the rise in spindle activity. The negative peak is followed by a positive potential coinciding with the time of highest spindle power. Thereafter, the DC potential shifts toward negativity again. During the time of peak spindle activity, the mean DC potential was 12–20 μV more positive than 500 msec before ($p < 0.001$) and after this time ($p < 0.001$, at both electrodes). Also, both the positive DC potential peak as well as the negative peaks before and after it were significant in comparison with the potential during the first 0.2 sec period of the averaging interval used as a baseline ($p < 0.01$, except for the negative peak after the spindle at Fz, which was $p < 0.05$). Interestingly, the negative DC shift immediately preceding the rise in spindle activity was at Fz significantly larger than the negative DC peak after the spindle (−13.8 ± 3.3 μV vs −6.9 ± 2.7 μV; $p < 0.05$).

The mean cross-correlation functions between the slow oscillatory EEG potential and the spindle rms signal during periods of SWS are shown in Figure 6. Although correlation coefficients were generally of moderate size, the cross-correlation function shows distinct and significant peaks ($p < 0.005$). In both channels, a positive peak value is located at a time lag of −100 msec, indicating that changes in the spindle rms signal tend to precede shifts in the corresponding direction of the slow oscillatory signal. The highest cross-correlation is negative and at a time shift of 400

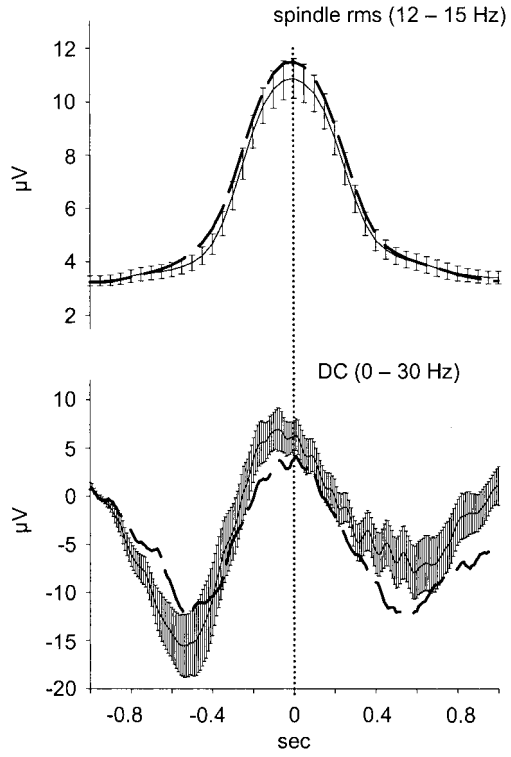

Figure 5. Grand means (across 13 subjects) of sleep-spindle-dependent changes in the DC potential. The mean ± SEM spindle rms signal (*top*) and DC potential (*bottom*) at Fz, both averaged time-locked to the spindle center, are shown. *Dashed lines* indicate respective mean values from Cz (without SEM). The *vertical dotted line* indicates the spindle center time used for time-locked averaging.

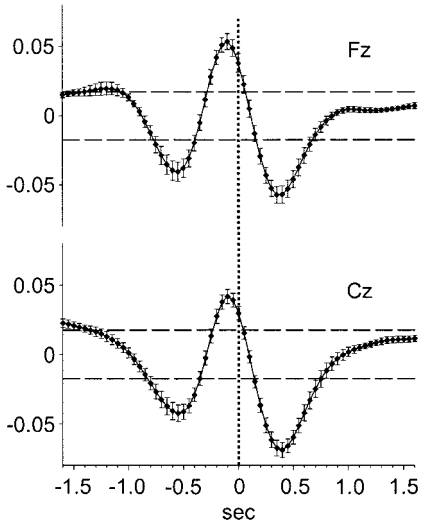

Figure 6. Mean ± SEM cross-correlation function between slow-oscillation signal and spindle rms signal across 13 subjects at Fz (*top*) and Cz (*bottom*). *Dashed horizontal lines* indicate a $p < 0.005$ level of significance. The *vertical dotted line* indicates the time lag of 0 sec.

msec, indicating that changes in the spindle rms signal occur 400 msec after changes in the slow-oscillation band signal in the opposite direction. This peak coefficient probably reflects the strong increase in spindle activity after the peak of the negative half-wave (Fig. 4*B*).

DISCUSSION

Results show that during human SWS, rhythmic activity in the 12–15 Hz spindle frequency range becomes grouped during slow oscillations (with a dominant frequency of 0.7–0.8 Hz). Wave-triggered averages of the spindle rms signal reveal suppressed spindle activity during slow negative half-waves and enhanced activity during positive half-waves. For the adjacent beta-frequency band (15–25 Hz), a similar although weaker modulation in the course of slow oscillations was observed. However, there were no similar dynamics expressed for the alpha (8–12 Hz) and theta (4–8 Hz) frequency bands. Complementing these observations, discrete spindles identified during non-REM stage 2 and stage 3 sleep were found to be preceded by a slow negative DC shift followed by a positive DC potential during the spindle. The temporal dynamics of these DC shifts were similar to slow oscillatory activity.

The averaged power spectrum of the DC-recorded EEG during SWS (stages 3 and 4) revealed a clear peak at ~0.7–0.8 Hz (Fig. 2). This frequency peak, which is distinctly <1 Hz, corresponds to the slow oscillation frequency reported previously in sleeping humans (Achermann and Borbély, 1997; Steriade and Amzica, 1998) and cats (Steriade et al., 1996). The small peak at ~0.25 Hz preceding the main 0.7–0.8 Hz peak in the frequency histogram depicted in Figure 2 might indicate the presence of a class of even slower oscillations (also see Steriade et al., 1993a). However, inspection of individual spectra revealed that in subjects showing a distinct peak of ~0.25 Hz, this was much less pronounced than the main 0.7–0.8 Hz peak. This agrees well with previous observations, in which subjects with abundant slow oscillations showed great peaks in the 0.7–0.8 Hz range, although peaks at somewhat longer periodicities may occur (Steriade and Amzica, 1998). The dominating frequency of 0.7–0.8 Hz also distinguishes the waves selected for our analysis from typical delta waves defined by faster frequencies between 1 and 4 Hz, although our spectra did not provide safe indications for the existence of a separate delta peak. Our algorithm detected the largest positive and negative deflections, with a duration of 0.125–1 sec in the 0.16–4 Hz filtered signal. This resulted in averaged half-waves with a length of 0.6–0.8 sec (Fig. 4*B*), which corresponds to a period length of 1.2–1.6 sec (i.e., a frequency of 0.62–0.83 Hz) for the oscillation underlying the averaged half-waves. Thus, the frequency content of the half-waves chosen for analysis here exactly fit the frequency range of 0.6–1 Hz used in previous reports to define and establish the existence of this slow oscillatory rhythm (Steriade and Amzica, 1998; Steriade, 1999). Along these lines, it seems justified to consider the half-waves of our study to be specific EEG manifestations of the slow oscillations originally described by Steriade et al. (1993a) in animals.

The animal data indicate that these slow waves have the virtue of grouping cortically recorded spindle activity and also faster oscillations in the beta and gamma frequency range (20–60 Hz). The present data extend this observation by showing a similar grouping of spindle activity in humans. Gamma activity was not the focus of this study, because it is prone to artifacts, primarily of muscular origin, in recordings of ongoing EEG activity from the human scalp. We did observe a significant modulation by slow oscillations of beta band activity, which like gamma activity is considered to reflect processing of representations. However, more distant cortical areas are involved in the generation of beta activity, and the synchronization properties are probably different from those of gamma activity (Kopell et al., 2000). Thus, an

intriguing question remains about whether gamma activity displays a similar modulation.

Our result of enhanced spindle power during surface-positive half-waves of slow oscillations is quite consistent with the underlying mechanisms of the grouping of spindle activity during slow rhythmic activity, as revealed in animals (Contreras et al., 1997; Destexhe et al., 1999; Steriade, 1999). These studies indicated that slow positive potential shifts recorded from the cortical surface correspond to extracellular depth potentials of negative polarity and to a prolonged depolarization of neocortical pyramidal cells. This depolarization is associated with increased firing, which drives the generation of spindle oscillations in thalamo-neocortical feedback loops (Contreras and Steriade, 1995; Steriade et al., 1996; Destexhe et al., 1999). In contrast, the surface-negative components of slow waves corresponding to intracellular hyperpolarization were associated with neuronal silence. This corresponds to the finding of suppressed spindle activity during slow negative half-waves in the present study. Thus, our results show that during non-REM SWS also in human surface EEG recordings, a consistent relationship of spindle activity with the depolarizing and hyperpolarizing phase of slow oscillations is distinguishable. A similar relationship could underlie the grouping of spindles dominating during sleep stage 2, which in previous studies was found to display a periodicity of ~4 sec (Achermann and Borbély, 1997; Marshall et al., 2000).

To obtain more accurate information with regard to the temporal relationships between slow oscillations and spindle activity, cross-correlation functions were calculated that revealed overall low coefficients with distinct and highly significant peaks of interest. There was a positive correlation between both time series with a peak at −100 msec, indicating that changes in spindle activity tend to precede those in the slow oscillatory signal. At first glance, this temporal relationship appears to be in contrast to findings in cats, indicating that the depolarizing component (i.e., surface-positive EEG component) of the slow oscillation is the factor driving the thalamic generation of spindle activity via corticothalamic volleys (Steriade and Amzica, 1998; Steriade, 1999). However, examination of Figure 4 indicates that although the slow positive half-wave starts at virtually the same time as the increase in spindle activity, spindle activity peaks and begins to decrease ~100 msec earlier than the slow positive half-wave. Thus, rather than a time lag in the onset of these two phenomena, the positive correlation at −100 msec reflects the fact that the duration of the depolarizing phase of slow oscillations during SWS obviously exceeds the duration of triggered spindle activity, the waning of which is regulated by separate mechanisms (Luthi and McCormick, 1998; Sejnowski and Destexhe, 2000). An additional although perhaps minor contribution of spindle activity to the positive EEG deflection of the slow oscillation may be considered in light of our finding that isolated spindles identified during non-REM sleep stages 2 and 3 coincided with a small but discrete positive DC potential. In animals, the induction of cortical spindle-like activity in conjunction with augmenting responses is found to be followed by secondary longer-lasting depolarizations that may add to the depolarizing part of the cortically generated slow oscillation (Steriade, 1993, 2001; Steriade et al., 1998). However, it should be noted that the slow oscillation can be recorded in athalamic animals in which spindles are absent (Steriade et al., 1993b).

The most pronounced peak in the cross-correlation function was of negative polarity and occurred at a time lag of 400 msec (Fig. 6). This peak has to be linked to the interesting fact that the highest spindle activity found in the present analysis was not that coinciding with slow positive half-waves but rather that following the peak of slow negative half-waves by ~400 msec (Fig. 4*B*). This distinct rebound enhancement in spindle activity after slow negative half-waves likely reflects postinhibitory rebound spike-bursts in thalamocortical neurons, as described by Contreras and Steriade (1995). They found that intracellularly recorded thalamocortical neurons at almost every cycle of the slow oscillation showed burst responses after their disfacilitation (and silenced firing) that correspond in time to the scalp-negative (depth-positive) wave [Contreras and Steriade (1995), their Figs. 8 and 9]. Also, the averaging of DC potentials time-locked to the center of spindles in sleep stages 2 and 3 revealed that the onset of spindles was preceded by a remarkably strong negative potential shift (Fig. 5). Together, these results indicate that the most pronounced enhancements of spindle activity occur a short time after phases of relatively strong hyperpolarization within cortical cells; this rebound spindle activity exceeds that observed during more depolarizing phases. This interpretation stresses the importance of previous hyperpolarization for the synchronizing influence of slow oscillations on spindle activity, which adds to the influence of cortical depolarization. This view is corroborated by the observation that strong rebound spindle activity after slow negative half-waves coincides with only a moderate positive slow oscillatory potential. Also, the slow negative half-waves in our analysis showed a steeper onset and a higher (absolute) peak amplitude than the positive half-waves.

Our data show a grouping of spindle activity coinciding with negative and positive parts of slow oscillations during human non-REM and SWS, which presumably reflect the inhibiting and driving forces of, respectively, hyperpolarizing and depolarizing phases of cortical cells on thalamically generated spindle activity. beta activity displayed a similar dynamic. Additional research is justified to clarify whether this pattern is relevant for the supposed iterative mechanisms of memory reprocessing during non-REM and SWS.

REFERENCES

Achermann P, Borbély AA (1997) Low-frequency (<1 Hz) oscillations in the human sleep electroencephalogram. Neuroscience 81:213–222.
Aeschbach D, Borbély AA (1993) All-night dynamics of the human sleep EEG. J Sleep Res 2:70–81.
Amzica F, Steriade M (1997) The K-complex: its slow (<1-Hz) rhythmicity and relation to delta waves. Neurology 49:952–959.
Bauer H, Korunka C, Leodolter M (1989) Technical requirements for high-quality scalp DC recordings. Electroencephalogr Clin Neurophysiol 72:545–547.
Buzsáki G (1998) Memory consolidation during sleep: a neurophysiological perspective. J Sleep Res 7 [Suppl 1]:17–23.
Buzsáki G, Bickford RG, Ponomareff G, Thal LJ, Mandel R, Gage FH (1988) Nucleus basalis and thalamic control of neocortical activity in the freely moving rat. J Neurosci 8:4007–4026.
Contreras D, Steriade M (1995) Cellular basis of EEG slow rhythms: a study of dynamic corticothalamic relationships. J Neurosci 15:604–622.
Contreras D, Steriade M (1996) Spindle oscillation in cats: the role of corticothalamic feedback in a thalamically generated rhythm. J Physiol (Lond) 490 [Suppl 1]:159–179.
Contreras D, Destexhe A, Steriade M (1997) Intracellular and computational characterization of the intracortical inhibitory control of synchronized thalamic inputs in vivo. J Neurophysiol 78:335–350.
De Gennaro L, Ferrara M, Bertini M (2000a) Effect of slow-wave sleep deprivation on topographical distribution of spindles. Behav Brain Res 116:55–59.
De Gennaro L, Ferrara M, Bertini M (2000b) Topographical distribution of spindles: variations between and within NREM sleep cycles. Sleep Res Online 3:155–160.
Destexhe A, Contreras D, Steriade M (1999) Spatiotemporal analysis of local field potentials and unit discharges in cat cerebral cortex during natural wake and sleep states. J Neurosci 19:4595–4608.
Dijk DJ, Hayes B, Czeisler CA (1993) Dynamics of electroencephalo-

graphic sleep spindles and slow wave activity in men: effect of sleep deprivation. Brain Res 626:190–199.
Gais S, Plihal W, Wagner U, Born J (2000) Early sleep triggers memory for early visual discrimination skills. Nat Neurosci 3:1335–1339.
Gais S, Mölle M, Helms K, Born J (2002) Learning-dependent increases in sleep spindle density. J Neurosci 22:6830–6834.
Kopell N, Ermentrout GB, Whittington MA, Traub RD (2000) Gamma rhythms and beta rhythms have different synchronization properties. Proc Natl Acad Sci USA 97:1867–1872.
Luthi A, McCormick DA (1998) Periodicity of thalamic synchronized oscillations: the role of Ca^{2+}-mediated upregulation of Ih. Neuron 20:553–563.
Marshall L, Mölle M, Fehm HL, Born J (1998) Scalp recorded direct current brain potentials during human sleep. Eur J Neurosci 10: 1167–1178.
Marshall L, Mölle M, Fehm HL, Born J (2000) Changes in direct current (DC) potentials and infra-slow EEG oscillations at the onset of the luteinizing hormone (LH) pulse. Eur J Neurosci 12:3935–3943.
Picton TW, Hillyard SA (1972) Cephalic skin potentials in electroencephalography. Electroencephalogr Clin Neurophysiol 33:419–424.
Plihal W, Born J (1997) Effects of early and late nocturnal sleep on declarative and procedural memory. J Cogn Neurosci 9:534–547.
Rechtschaffen A, Kales A (1968) A manual of standardized terminology, techniques and scoring system for sleep stages of human subjects. Washington, DC: National Institutes of Health 204.
Schimicek P, Zeitlhofer J, Anderer P, Saletu B (1994) Automatic sleep-spindle detection procedure: aspects of reliability and validity. Clin Electroencephalogr 25:26–29.
Sejnowski TJ, Destexhe A (2000) Why do we sleep? Brain Res 886: 208–223.
Siapas AG, Wilson MA (1998) Coordinated interactions between hippocampal ripples and cortical spindles during slow-wave sleep. Neuron 21:1123–1128.
Steriade M (1993) Cellular substrates of brain rhythms. In: Electroencephalography: basic principals, clinical applications, and related fields. (Niedermeyer E, Lopes da Silva F, eds), pp 27–62. Baltimore: Williams and Wilkins.
Steriade M (1999) Coherent oscillations and short-term plasticity in corticothalamic networks. Trends Neurosci 22:337–345.
Steriade M (2001) The intact and sliced brain. Cambridge, MA: MIT.
Steriade M, Amzica F (1998) Coalescence of sleep rhythms and their chronology in corticothalamic networks. Sleep Res Online 1:1–10.
Steriade M, Nuñez A, Amzica F (1993a) A novel slow (<1 Hz) oscillation of neocortical neurons *in vivo*: depolarizing and hyperpolarizing components. J Neurosci 13:3252–3265.
Steriade M, Nuñez A, Amzica F (1993b) Intracellular analysis of relations between the slow (<1 Hz) neocortical oscillation and other sleep rhythms of the electroencephalogram. J Neurosci 13:3266–3283.
Steriade M, Contreras D, Amzica F (1994) Synchronized sleep oscillations and their paroxysmal developments. Trends Neurosci 17:199–208.
Steriade M, Amzica F, Contreras D (1996) Synchronization of fast (30–40 Hz) spontaneous cortical rhythms during brain activation. J Neurosci 16:392–417.
Steriade M, Timofeev I, Grenier F, Dürmüller N (1998) Role of thalamic and cortical neurons inaugmenting responses and self-sustained activity: dual intracellular recordings *in vivo*. J Neurosci 18:6425–6443.
Sutherland GR, McNaughton B (2000) Memory trace reactivation in hippocampal and neocortical neuronal ensembles. Curr Opin Neurobiol 10:180–186.